Inorganica Chimica Acta 384 (2012) 324–332

Contents lists available at SciVerse ScienceDirect

Inorganica Chimica Acta

journal homepage: www.elsevier.com/locate/ica

Crystal structure, biological studies of water-soluble rare earth metal complexes with an ofloxacin derivative

Min Xu [a,b], Yu-cui Zhang [b], Zhi-hong Xu [c,*], Zheng-zhi Zeng [b,*]

[a] College of Earth and Environmental Sciences, Lanzhou University, Lanzhou 730000, China
[b] Key Laboratory of Nonferrous Metals Chemistry and Resources Utilization of Gansu Province, Lanzhou University, Lanzhou 730000, China
[c] College of Chemistry and Chemical Engineering, Xuchang University, Xuchang 461000, China

ARTICLE INFO

Article history:
Received 29 December 2010
Received in revised form 14 November 2011
Accepted 15 December 2011
Available online 24 December 2011

Keywords:
Ofloxacin
Ln(III) complexes
DNA interaction
DNA cleavage
Antioxidant activity

ABSTRACT

Two new water-soluble solid complexes [PrL $(NO_3)_2(CH_3OH)$] (NO_3), $[NdL(NO_3)_2(CH_3OH)](NO_3)$(L = 9-fluoro-2,3-dihydro-3-methyl-10-(4-methyl-1-piperaziny)-7-oxo-7H-pyrido [1,2,3-de]-1,4-benzoxazine-6-carbaldehyde benzoyl hydrazone) have been synthesized by the reaction of Ln(III) nitrate with an ofloxacin derivative. The crystal structures of $[PrL(NO_3)_2(CH_3OH)](NO_3)$ and $[NdL(NO_3)_2(CH_3OH)](NO_3)$ were determined by single-crystal X-ray diffraction. The interactions of the ligand and Ln(III) complexes with calf thymus DNA (CT DNA) have been investigated by UV–Vis (UV–Vis) spectra, ethidium bromide (EB) displacement experiments, circular dichroism (CD) spectra, cyclic voltammetry (CV) and viscosity measurements. Experimental results indicated that Ln(III) complexes and ligand could bind to CT DNA via the intercalation mode and that the binding affinities of Ln(III) complexes are higher than that of free ligand. In addition, Ln(III) complexes could cleave pBR322 DNA in the presence and the absence of reductant. The free ligand did not show any DNA-cleaving abilities. Furthermore, the antioxidant activity of the ligand and Ln(III) complexes was determined by superoxide and hydroxyl radical scavenging methods in vitro, which indicate that the Ln(III) complexes exhibit more effective antioxidant activity than the ligand alone.

1. Introduction

Metal complexes that bind and cleave DNA under physiological conditions are of current interests for their varied applications in nucleic acid chemistry, namely, as models for restriction enzymes, footprinting agents, and therapeutic agents [1–7]. Basically, the complex bound to DNA through three non-covalent modes: intercalation, groove binding and external static electronic effects. Understanding the DNA binding properties of metal complexes is in the hope of developing novel probes of nucleic acid structure, DNA footprinting and sequence-specific cleaving agents, antitumor drugs, etc. [8–10]. DNA cleavage could proceed via hydrolytic or oxidative pathways. Hydrolytic cleavage of DNA involves hydrolysis of the phosphodiester bond generating fragments that could be rejoined making the compounds as models for restriction enzymes having utility in genomic research. Ln(III), Cu(II) and Zn(II) complexes are better suited for the hydrolysis of DNA due to the strong Lewis acid properties of these metal ions [3–6]. Oxidative cleavage of DNA generally causes degradation of the sugar and/or base moiety thus making the process suitable for foot-printing and therapeutic applications. Therefore, much of the attention has been targeted on the design of metal-based complexes, which can bind and cleave DNA.

Quinolones (quinolone-carboxylic acids or 4-quinolones) are a group of synthetic antibacterial agents that act as antibacterial drugs by inhibiting effectively DNA replication and are commonly used as treatment for many infections [11]. Ofloxacin ((±)9-fluoro-2,3-dihydro-3-methyl-10-(4-methyl-1-piperaziny)-7-oxo-7*H*-pyrido[1,2,3-de]-1,4-benzoxazine-6-carboxylic acid; Fig. 1) is one of the most frequently used fluorinated quinolones antibiotics in the world [12]. It has a broad spectrum of activity against gram-positive, gram-negative aerobic, facultatively anaerobic bacteria, chlamydiae, and some related organisms, such as mycoplasmas or mycobacteria [13]. Moreover, Schiff bases play an important role in bioinorganic chemistry as they exhibit remarkable biological activity. The acid hydrazides R–CO–NH–NH_2, a class of Schiff base, their corresponding aroylhydrazones, R–CO–NH–N=CH–R′, and the dependence of their mode of chelation with metal ions present in living systems have been of significant interest [14–18].

So we synthesized and characterized the salicylaldehyde (±)9-fluoro-2,3-dihydro-3-methyl-10-(4-methyl-1-piperaziny)-7-oxo-7*H*-pyrido [1 , 2,3-de]-1,4-benzoxazine-6-carboxylhydrazone and its Pr(III) and Nd (III) complexes. Spectroscopy, CV and viscosity measurements showed that the ligand and its Ln(III) complexes can interact with CT DNA through

* Corresponding authors. Tel.: +86 931 8912582; fax: + 86 374 4369257.
E-mail addresses: xuzhihong1980@yahoo.com.cn (Z.-h. Xu), zengzhzh@yahoo.com.cn (Z.-z. Zeng).

0020-1693/$ - see front matter © 2011 Elsevier B.V. All rights reserved.
doi:10.1016/j.ica.2011.12.031

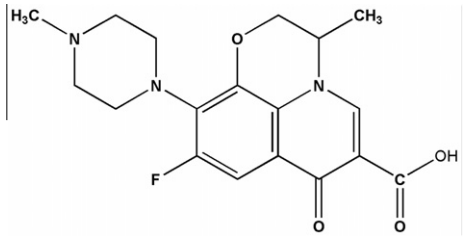

Fig. 1. The structure of ofloxacin.

intercalation, and Ln(III) complexes present stronger affinities to CT DNA than ligand. Gel electrophoresis experiments showed Ln(III) complexes can promote the DNA cleavage more efficiently than ligand under physiological conditions. In addition, the two water-soluble Ln(III) complexes are found to possess potentially antioxidant activities.

2. Experimental

2.1. Materials

Nitroblue tetrazolium (NBT), methionine (MET), vitamin B_2 ($VitB_2$), Ethidium bromide (EB), and CT DNA were purchased from Sigma Chemical Co. EDTA, $NaBH_4$, ethyl acetate, $M(NO_3)_3{\cdot}6H_2O$ [M = Pr(III), Nd(III)] were produced in China. All chemicals used were of analytical grade. EDTA–Fe(II) and KH_2PO_4–K_2HPO_4 buffers were prepared with doubly distilled water. All the experiments involved with the interaction of ligand and complexes with CT DNA were carried out in doubly distilled water buffer containing Tris [tris(hydroxymethyl)-aminomethane] (5 mM) and NaCl (50 mM) and adjusted to pH 7.2 with hydrochloric acid. Solution of CT DNA in the buffer gave ratios of UV–Vis absorbance of about 1.8–1.9:1 at 260 and 280 nm, indicating that the CT DNA was sufficiently free of protein [19]. The CT DNA concentration per nucleotide was determined spectrophotometrically by employing an extinction coefficient of 6600 $m^{-1}\,cm^{-1}$ at 260 nm [20].

2.2. Physical measurements

Carbon, hydrogen and nitrogen were determined using an Elemental Vario EL analyzer. The melting point of the ligand was determined on a Beijing XT4-100X microscopic melting point apparatus (the thermometer was not calibrated). The IR spectra were obtained in KBr disks on a Therrno Mattson FTIR spectrophotometer in the 4000–400 cm^{-1} region. ^1H NMR spectra were recorded on a Varian VR 200 MHz spectrometer in DMSO-d^6 with TMS (tetramethylsilane) as internal standard. Mass spectra were performed on an APEX II FT-ICR MS instrument using methanol as mobile phase. The UV–Vis spectra were recorded on a Shimadzu UV-240 spectrophotometer. Fluorescence measurements were recorded on a Hitachi RF-4500 spectrofluorophotometer at room temperature. The antioxidant activity was performed in DMF solution with a 721-E spectrophotometer.

2.3. DNA binding experiments

2.3.1. Viscosity measurements

Viscosity experiments were conducted on an Ubbdlodhe viscometer, immersed in a thermostated water-bath maintained to 25.0 °C. Titrations were performed for the complexes (1–5 μM), and each compound was introduced into DNA solution (5 μM) present in the viscometer. Data were presented as $(\eta/\eta_c)^{1/3}$ versus the ratio of the concentration of the compound and DNA, where η is the viscosity of DNA in the presence of compound and η_0 is the viscosity of DNA alone. Viscosity values were calculated from the observed flow time of DNA containing solution corrected from the flow time of buffer alone (t_0), $\eta = t - t_0$ [21].

2.3.2. Electronic absorption titration

An absorption titration experiment was performed by maintaining 10 μM compounds and varying the concentration of nucleic acid. While measuring the absorption spectra, an equal amount of CT DNA was added to both the compound solution and the reference solution to eliminate the absorbance of CT-DNA itself. From the absorption titration data, the binding constant was determined using the following Eq. (1) [22]:

$$[DNA]/(\varepsilon_a - \varepsilon_f) = [DNA]/(\varepsilon_b - \varepsilon_f) + 1/K_b(\varepsilon_b - \varepsilon_f) \quad (1)$$

where [DNA] is the concentration of DNA in base pairs, ε_a corresponds to the extinction coefficient observed (A_{obsd}/[M]), ε_f corresponds to the extinction coefficient of the free compound, ε_b is the extinction coefficient of the compound when fully bound to DNA, and K_b is the intrinsic binding constant. The ratio of slope to intercept in the plot of $[DNA]/(\varepsilon_a - \varepsilon_f)$ versus [DNA] gives the values of K_b.

2.3.3. EB displacement experiments

Further evidence for complexes and ligand binding to DNA via intercalation is given through the emission quenching experiment. EB is a common fluorescent probe for DNA structures and has been employed in examinations of the mode and process of metal complex binding to DNA [23]. A 2.0 mL solution of 4 μM DNA and 0.32 μM EB (at saturation binding levels) was titrated by 0–110 μM complexes and ligand (λ_{ex} = 525 nm, λ_{em} = 520.0–650.0 nm). Quenching data were analyzed according to the Stern–Volmer equation (Eq. (2)) which could be used to determine the fluorescent quenching mechanism [24]:

$$F_0/F = K_{SV}[Q] + 1 \quad (2)$$

where F_0 is the emission intensity in the absence of quencher, F is the emission intensity in the presence of quencher, K_{SV} is the quenching constant, and [Q] is the quencher concentration. The shape of Stern–Volmer plots can be used to characterize the quenching as being predominantly dynamic or static. Plots of F_0/F versus [Q] appear to be linear and K_{SV} depends on temperature.

2.3.4. CD spectra

The CD spectra were recorded on an Olos RSM 1000 at increasing complex/DNA ratio (r = 0.0, 0.5). Each sample dissolved in water was scanned in the range of 220–320 nm. A CD spectrum was generated which represented the average of three scans from which the buffer background had been subtracted. The concentration of DNA was 1.0×10^{-4} M.

2.3.5. Cyclic voltammetry experiments

Cyclic voltammetry experiments were performed at room temperature under an inert atmosphere (N_2) with a conventional three-electrode electrochemical cell, and using a CHI-420 electrochemical workstation (made in Shanghai, China). The three-electrode system used in this work consists of a glassy carbon electrode as working electrode, a saturated calomel electrode (SCE) as reference electrode and a Pt foil auxiliary electrode. Solution was prepared by dissolving the complexes in N,N-dimethyl formamide (DMF) and 100 mM $NaClO_4$ was used as supporting electrolyte.

2.4. DNA cleavage experiments

The cleavage of pBR322 DNA was studied by agarose gel electrophoresis. The concentration of the complexes in DMF or the

additives in buffer corresponded to the quantity in 2 μl stock solution after dilution to the 20 μl final volume using TBE buffer [0.045 M tris(hydroxymethyl)aminomethane (tris), 0.045 M boric acid, and 1 mM EDTA, pH 8.3]. The solution path length in the sample vial was ~5 mm. Each sample was incubated for 13 h at 37 °C and the samples were analyzed by electrophoresis for 1 h at 100 V on a 0.8% agarose gel in TBE buffer. The gel was stained with 1 mg/ml ethidium bromide and photographed on an Alpha Innotech IS-5500 fluorescence chemiluminescence and visible imaging system. Mechanistic studies were carried out using different additives (NaN_3, 0.1 mM; L-Histidine, 0.1 mM; DMSO, 2 μL; EtOH, 2 μL;) prior to the addition of the complex.

2.5. Antioxidant activity

Hydroxyl radical (HO·) scavenging activity through the Fenton reaction [25]. The solution of the compound to be tested was prepared in DMF. The tested samples contained 1 ml of 0.15 M phosphate buffer (pH 7.4), 1 ml of 40 $\mu g\,ml^{-1}$ safranin, 1 ml of 1.0 mM EDTA–Fe(II), 1 ml of 3% H_2O_2, and 0.5 ml of the solution of the tested compound (prepared as a series dilutions of the tested compound). The reaction mixtures were incubated at 37 °C for 60 min in a water-bath. The absorbances of the samples and a control were measured at 520 nm. The suppression ratio for OH^- was calculated from the following Eq. (3).

$$\text{Suppression ratio} = (A_{sample} - A_{blank})/(A_{control} - A_{blank}) \quad (3)$$

where A_{sample} is the absorbance of the sample in the presence of the tested compound, A_{blank} is the absorbance of the blank in the absence of the tested compound and $A_{control}$ is the absorbance in the absence of the tested compound and EDTA–Fe (II). IC_{50} value was introduced to denote the molar concentration of the tested compound which caused good inhibitory or scavenging effect on radicals.The superoxide radicals ($O_2^{-}\cdot$) were produced by the MET/$VitB_2$/NBT system [26]. The amount of $O_2^{-}\cdot$ and suppression ratio for $O_2^{-}\cdot$ can be calculated by measuring the absorbance at 560 nm. The solution of MET, $VitB_2$, and NBT were prepared in a 0.067 M phosphate buffer (pH 7.8) while avoiding light. The tested compounds were dissolved in DMF. The 5 ml reaction mixture contained MET (0.01 M), NBT (4.6×10^{-5} M), $VitB_2$ (3.3×10^{-6} M), and the tested compound. After illuminating the solution with a fluorescent lamp at 30 °C for 30 min, the absorbance (A_i) of the samples were measured at 560 nm. The sample without the tested compound was used as the control and its absorbance was used as A_0. The suppression ratio for $O_2^{-}\cdot$ was calculated from the following Eq. (4):

$$\text{Suppression ratio} = (A_0 - A_i)/A_0 \quad (4)$$

where A_i is the absorbance in the presence of ligand or its complexes and A_0 is the absorbance in the absence of ligand or its complexes.

2.6. Preparation of the ligand

Ofloxacin (1.88 g, 5 mmol) was esterified to 9-fluoro-2,3-dihydro-3-methyl-10-(4-methyl-1-piperaziny)-7-oxo-7H-pyrido[1,2,3-de]-1,4-benzoxazine-6-carboxylate, treatments of the esters with $N_2H_4{\cdot}H_2O$ (3 ml) gave the corresponding hydrazine. A methanol solution (15 ml) containing 2-hydroxybenzaldehyde (611 mg, 5 mmol) was added to another methanol solution (10 ml) containing the above hydrazine (188 mg, 5 mmol). The mixture was refluxed for 3 h with stirring and a yellow solid was separated out. After cooling to room temperature, the precipitate was filtered, and washed with ethanol to give the ligand. Yield 86% (Fig. 2).

Ester: white solid, m.p. 238 °C-240 °C, ^{1}H NMR (CD_3OH, 400 MHz) δ (ppm): 1.432–1.449 (3H, d, J = 6.8 Hz, $-CH_3$), 2.361–2.375(3H, d, J = 5.6 Hz, $-N-CH_3$), 2.642 (4H, s, 1′,4′ –H), 3.230-3.238(1H, m, 2–H), 3.325–3.336(4H, d, 2′,3′ –H), 4.331–4.535(2H, m, 1–H), 7.360–7.391(1H, d, 3–H), 8.511(1H, s, 7–H).

Hydrazine: yellowish solid, m.p. 200–202 °C, ^{1}H NMR (CD_3OH, 400 MHz) δ (ppm): 1.462–1.478 (3H, d, J = 6.4 Hz, $-CH_3$), 2.290(3H, s, $-N-CH_3$), 2.526 (4H, s, 1′,4′ –H), 3.229–3.236(1H, m, 2–H), 3.261–3.333(4H, d, 2′,3′ –H), 4.289–4.444(2H, m, 1–H), 7.305–7.336(1H, d, 3–H), 8.559(1H, s, 7–H).

Ligand: $C_{25}H_{26}FN_5O_4$, white solid, m.p. 264–266 °C, ^{1}H NMR (DMSO-d^6, 300 MHz) δ (ppm): 1.416–1.438(3H, d, J = 6.6 Hz, $-CH_3$), 2.207–2.237 (3H, d, J = 9.0 Hz, $-N-CH_3$), 2.479–2.503 (4H, m, 1′,4′ –H), 3.257–3.425 (5H, m, 2–H , 2′,3′ –H), 4.331–4.552 (2H, m, 1–H), 4.896(1H, s, –OH), 6.893-7.579 (4H, m, 7–H, 1′,2′,3′ –H), 8.608–8.638(1H, d, J = 9 Hz, 4′ –H), 8.876–8.905(1H, d, J = 8.7 Hz, 3–H)11.277 (1H, s, –CH=N). FAB-MS: m/z = 480.1 $[M+H]^+$. *Anal.* Calc. for $C_{25}H_{26}FN_5O_4$: C, 62.66; H, 5.50; N, 14.65. Found: C, 62.62; H, 5.47; N, 14.61%. IR υ_{max} (cm^{-1}): υ(N–H): 3443, ν(hydrazonic) C=O: 1664, υ(C=N): 1610. UV (Tris–HCl 5 mM, pH 7.2); $\varepsilon = 2.80 \times 10^4$ (λ = 302 nm); $\varepsilon = 2.29 \times 10^4$ (λ = 338 nm).

2.7. Preparation of the complexes

2.7.1. Pr(III) complex

Ligand (119 mg, 0.25 mmol) and NaOH (10 mg, 0.25 mmol) was mixed in 15 ml CH_3OH under stirring for 0.5 h at 60 °C, then $Pr(NO_3)_3{\cdot}6H_2O$ (131 mg, 0.3 mmol) was added into the reaction mixtures. The mixtures were refluxed and stirred continuously for 3 h. After cooling to room temperature, a yellow precipitate, Pr(III) complex was centrifugalized, washed with methanol and dried in vacuum over 24 h. Yield: 81%. *Anal.* Calc. for $C_{52}H_{58}F_2N_{16}O_{28}Pr_2$: C, 37.11; H, 3.52; N, 13.34. Found: C, 37.08; H, 3.46; N, 13.29%. IR υ_{max} (cm^{-1}): υ(N–H): 3384, υ(C=O): 1630, υ(C=N): 1543, $\upsilon(NO_3)$: 1385. UV (Tris–HCl 5 mM, pH 7.2); $\varepsilon = 3.57 \times 10^4$ (λ_{max} = 303 nm).

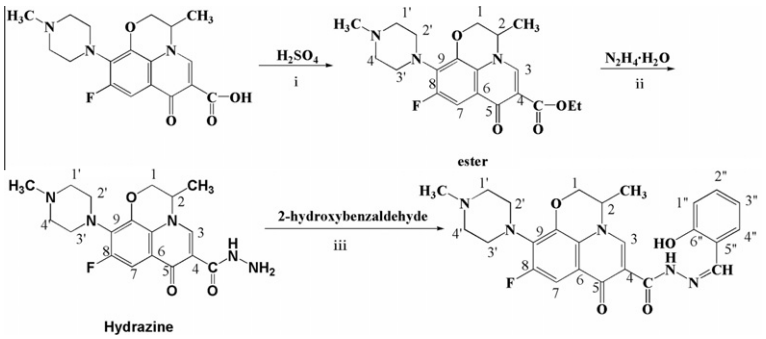

Fig. 2. The synthetic route of the ligand: (i) C_2H_5OH, reflux, 20 h; (ii) C_2H_5OH, reflux, 4 h; (iii) CH_3OH, reflux, 3 h.

Table 1
Crystal data and structure refinement of Ln(III) complexes.

	Pr(III) complex	Nd(III) complex
Empirical formula	$C_{52}H_{58}F_2N_{16}O_{28}Pr_2$	$C_{52}H_{58}F_2N_{16}O_{28}Nd_2$
Formula weight	1674.96	1681.62
Temperature (K)	293(2)	293(2)
λ (Å)	0.71073	0.71073
Crystal system, space group	monoclinic, $P2(1)/n$	monoclinic, $P2(1)/n$
Unit cell dimensions		
a (Å)	8.161(2)	8.3040(17)
b (Å)	16.084(4)	16.492(3)
c (Å)	24.062(7)	24.626(5)
α (°)	90	90
β (°)	92.741(4)	92.68(3)
γ (°)	90	90
V (Å^3)	3154.7(15)	3368.9(12)
Z	2	2
Calculated density (g/cm^3)	1.763	1.658
Absorption coefficient (mm^{-1})	1.633	1.624
$F(000)$	1684	1688
Crystal size (mm)	0.41 × 0.36 × 0.31	0.37 × 0.35 × 0.32
θ Range for data collection (°)	1.52–25.50	2.55–26.09
Index ranges	$-9 \leqslant h \leqslant 9$ $-15 \leqslant k \leqslant 19$ $-25 \leqslant l \leqslant 29$	$-10 \leqslant h \leqslant 9$ $-17 \leqslant k \leqslant 19$ $-28 \leqslant l \leqslant 29$
Reflections collected/unique	16037/5861	17260/6235
Refinement method	full-matrix least-squares on F^2	full-matrix least-squares on F^2
Goodness-of-fit (GOF) on F^2	1.24	1.023
Final R indices [$I > 2\sigma(I)$]	R_1 = 0.0488, wR_2 = 0.0569	R_1 = 0.0323, wR_2 = 0.0741
R indices (all data)	R_1 = 0.1016, wR_2 = 0.0630	R_1 = 0.0474, wR_2 = 0.0806
Largest diff. peak and hole (e Å^{-3})	1.068 and −1.050	0.87 and −0.50

2.7.2. Nd(III) complex

According to the same method, Nd(III) complex were prepared from equimolar amounts of $Nd(NO_3)_3{\cdot}6H_2O$ and ligand. Yield 78%. *Anal.* Calc. for $C_{52}H_{58}F_2N_{16}O_{28}Nd_2$: C, 37.13; H, 3.53; N, 13.24. Found: C, 37.11; H, 3.45; N, 13.20%. IR υ_{max} (cm^{-1}): υ(N–H): 3382, υ(C=O): 1627, υ(C=N): 1542, $\upsilon(NO_3)$: 1383. UV (Tris–HCl 5 mM, pH 7.2); $\varepsilon = 3.60 \times 10^4$ (λ_{max} = 304 nm).

2.8. X-ray crystallography

The single crystals of two water-soluble complexes were gained in the methanol using diffusing method. Details of the crystal parameters, data collection and refinements are listed in Table 1. A yellow crystal of Pr(III) complex was determined on a BRUKER SMART 1000 CCD diffractometer equipped with a graphite crystal monochromatized Mo Kα radiation (λ = 0.71073 Å) at 298(2) K. The intensity data were collected by the ω scan mode within $1.87° < \theta < 26.09°$ for hkl ($-9 \leqslant h \leqslant 9$, $-15 \leqslant k \leqslant 19$, $-25 \leqslant l \leqslant 29$) in the monoclinic system. Data were collected at 298(2) K using Mo Kα radiation (λ = 0.71073 Å). A light yellow crystal of Nd(III) complex was also measured. Data were collected at 298(2) K using Mo Kα radiation (λ = 0.71073 Å).The intensity data were collected by the ω scan mode within $2.55° < \theta < 26.09°$ for hkl ($-10 \leqslant h \leqslant 9$, $-17 \leqslant k \leqslant 19$, $-28 \leqslant l \leqslant 29$) in the monoclinic system. The structure was solved by direct methods. The positions of non-hydrogen atoms were determined from successive Fourier syntheses. The hydrogen atoms were placed in their geometrically calculated positions. The positions and anisotropic thermal parameters of all non-hydrogen atoms were refined on F^2 by full-matrix least-squares techniques with the SHELX-97 program package [27].

3. Results and discussion

The complexes are air-stable for extended periods and soluble in DMSO, DMF and water; slightly soluble in ethanol or methanol; insoluble in benzene or diethyl ether.

3.1. Infrared spectra

IR spectra usually provide a lot of valuable information on coordination reactions. The IR spectra of the two complexes are very similar. The υ(N–H) appears at 3443 cm^{-1} for ligand, and this peak shifts at 3384 cm^{-1} or so for complexes. The band at 1665 cm^{-1} in the spectrum of ligand, related to the υ(C=O) pyridine, shifts up to 1530–1527 cm^{-1} for Pr (III) complex and Nd(III) complex, and $\Delta\upsilon$ (ligand–complexes) is equal to 35 and 38 cm^{-1}, respectively. The band at 592 cm^{-1} or so for Ln(III) complexes is assigned to υ(M–O) [28]. These shifts demonstrate that the oxygen of carbonyl has formed a coordinative bond with the rare earth ions. The band at 1610 cm^{-1} for the free ligand is assigned to the υ(C=N) stretch, which shifts to 1542 cm^{-1} or so for the complexes. Weak bands at 430 cm^{-1} or so for Ln(III) complexes are assigned to υ(M–N) [29]. These results further confirm that the nitrogen of the imino group bonds to the rare earth ions. The absorption bands of the coordinated nitrates were observed at about 1475 (υ_{as}) and 840 (υ_s) cm^{-1}. The υ_3 (E') free nitrates appear at 1385 cm^{-1} or so in the spectra of the complexes. In addition, the separation of the two highest frequency bands $|\upsilon_4 - \upsilon_1|$ is approximately 160 cm^{-1}, which indicates the bidentate ligand feature of the coordinated NO_3^- in the complexes [30].

3.2. X-ray structural characterization

Ofloxacin complexes with Cu(II), Co(II), Ni(II), Mg(II), Zn(II) and Ru(II) salts have been reported. From their X-ray crystal data, it was found that, the metal ion is chelate bonded to the ofloxacin in the complexes through ring carbonyl and one of the carboxylic oxygen atoms [31–35]. In this work, we have prepared an ofloxacin derivative with the hydrazone group. So the coordination with ofloxacin in our complexes is different from that of the complexes described above.

The coordination of the hydrazone with Ln(III) results in the formation of a five membered (LnNNCO) and a six-membered (LnNCCCO) chelating rings in which the lanthanide ion is nine-coordinate. The Pr(III) complex and Nd(III) complex crystallized in a monoclinic lattice with a space group $P2(1)/n$. ORTEP drawings with the atom numbering scheme for $[PrL(NO_3)_2(CH_3OH)](NO_3)$ and $[NdL(NO_3)_2(CH_3OH)](NO_3)$ are shown in Figs. 3 and 4. This crystal structure of binuclear $[PrL(NO_3)_2(CH_3OH)](NO_3)$ complex with a 1:1 metal-to-ligand stoichiometry and nine-coordination is similar to that of $[NdL(NO_3)_2(CH_3OH)](NO_3)$. Ligand acts as a monad tetradentate ligand, binding to Ln(III) through the phenolate oxygen atom, and the C=N group, O=C–NH– group of the benzoylhydrazine side chain. In addition, one nitrate (bidentate) is binding to the ligand-plane from one side to the metal ion, while another nitrate and CH_3OH are binding from the other. Dimerization of this monomeric unit occurs through the quinolone oxygen atoms.

In Pr(III) complex, five types of Ln–ligand interactions were found. The Pr (1)–O (11) hydrazonic distance was 2.482(3) Å, while the Pr (1)–O (12A) hydroxyl distances were found to be 2.261(3) Å. The Pr–imine distances were found to be 2.648(4) Å, for Pr (1)–N (4). The two bidentate nitrates were found to be 2.556(3) Å and

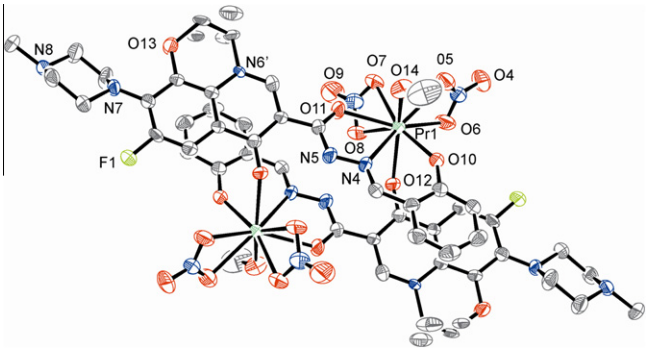

Fig. 3. The molecular structure and partially labeling of Pr(III) complex.

2.553(4) Å for Pr (1)–O (5), Pr (1)–O (6) and 2.646(4) Å and 2.597(4) Å for Pr (1)–O (7) and Pr (1)–O (8). Finally, methanol was found at 2.464(4) Å, Pr (1)–O (14). The Nd(III) complex also has five types of Ln–ligand interatomic interactions. The Nd (1)–O (11) hydrazonic distance was 2.519(3) Å, while the Nd (1)–O (12A) hydroxyl distances were found to be 2.507(3) Å. The Nd–imine distances were found to be 2.687(3) Å, for Nd (1)–N (4). The two bidentate nitrates were found to be 2.595(3) Å and 2.587(3) Å for Nd (1)–O (5), Nd (1)–O (6) and 2.692(3) Å and 2.642(3) Å for Nd (1)–O (7) and Nd (1)–O (8). Finally, methanol was found at 2.503(3) Å, Nd (1)–O (14). The Ln–O hydroxyl distance (2.261 Å Pr and 2.507 Å Nd) is significantly shorter than the average hydrazonic Ln–O distance (2.482 Å Pr and 2.519 Å Nd), which suggests that the hydroxyl bond is stronger than the hydrazonic bond. This is in agreement with the IR spectral data.

3.3. DNA binding studies

3.3.1. Viscosity titration measurements

Measurements of DNA viscosity that is sensitive to DNA length are regarded as the least ambiguous and the most critical tests of binding in solution in the absence of crystallographic structural data [36,37]. A classical intercalation mode demands that the DNA helix must lengthen as base pairs are separated to accommodate the binding complexes, leading to the increase of DNA viscosity, as for the behaviors of the known DNA intercalators [38]. In contrast, a partial and/or non-classical intercalation of the complex could bend (or kink) the DNA helix, reducing its viscosity concomitantly [39]. The effects of all the compounds on the viscosity of CT DNA are shown in Fig. 5. With the ratios of the investigated compounds to DNA increase, the relative viscosities of DNA increase steadily, indicating that there exist intercalations between ligand and rare earth metal complexes with DNA helix. In addition, the relative viscosities of DNA increase with the order of Pr(III) complex ≈ Nd(III) complex > ligand. These orders suggest the extents of the unwinding and lengthening of DNA helix by compounds and the affinities of compounds binding to DNA, which may be due to the larger coplanar structures of rare earth metal complexes than those of ligand. Intercalation has been traditionally associated with molecules containing fused bi/tricyclic ring structures [40], so it is logical that all the large coplanar Ln(III) complexes containing fused multiple cyclic ring structures and the ligand containing fused tricyclic ring structures can bind to DNA through intercalations.

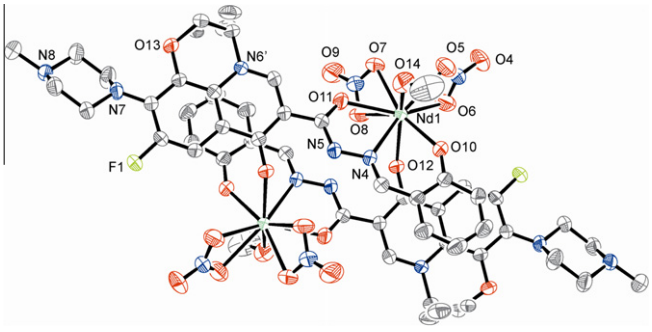

Fig. 4. The molecular structure and partially labeling of Nd(III) complex.

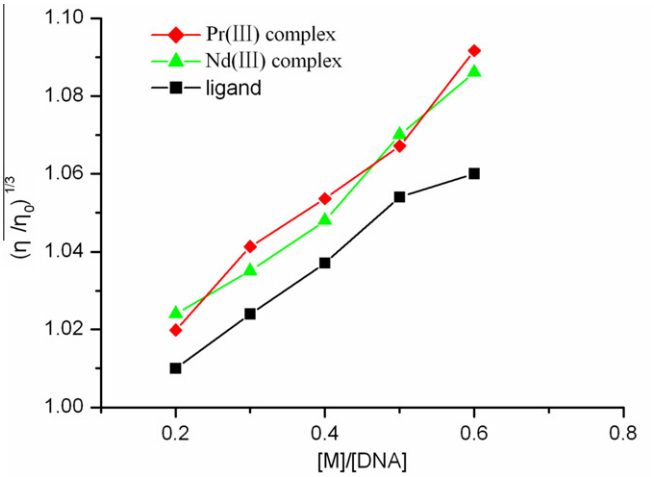

Fig. 5. Effects of increasing amounts of the investigated compounds on the relative viscosity of CT DNA in 5 mmol Tris–HCl buffer solution (pH 7.20) containing 50 mmol NaCl at 25(±0.1) °C.

3.3.2. Electronic absorption titration

Electronic absorption spectroscopy is one of the most useful techniques for DNA-binding studies of metal complexes. The changes observed in the UV–Vis spectra upon titration may give evidence of the existing interaction mode, since a hypochromism due to $\pi \rightarrow \pi^*$ stacking interactions may appear in the case of the intercalative binding mode [41], while red-shift (bathochromism) may be observed when the DNA duplex is stabilized [42].

Upon successive additions of CT DNA, the UV–Vis absorption bands of ligand show two types of progressive hypochromism of 42.36% at 306 nm and 44.21% at 339 nm, respectively, with a 0, 2 nm red shifts of absorption bands in the region of 306–339 nm (Fig. 6). Similarly, upon successive additions of CT DNA, the UV–Vis absorption bands of Pr (III) complex and Nd (III) complex show another progressive hypochromism of 85.01% at 303 nm and 86.94% at 304 nm, respectively. Absorption titration can monitor the interaction of a compound with DNA. The obvious hypochromism and red shift are usually characterized by the noncovalently intercalative binding of compound to DNA helix, due to the strong stacking interaction between the aromatic chromophore of the compound and base pairs of DNA [43,44]. So the above phenomena imply that the free ligand and Ln(III) complexes interact with CT DNA quite probably by intercalating the compounds into the DNA base pairs.

On the other hand, the magnitude of hypochromism is parallel to the intercalative strength and the affinity of a compound binding to DNA [45]. The appreciable hypochromisms of ligand and Ln(III) complexes intercalating to DNA present the order of Pr (III) complex ≈ Nd(III) complex > ligand, which are in good agreement with the orders of viscosity titration results.

K_b is a useful tool to calculate the magnitude of the binding strength of compounds with CT DNA and represents the binding constant per DNA base pair the binding constant. Plots of [DNA]/

($\varepsilon_a - \varepsilon_f$) versus [DNA] are shown in Fig. 7 and binding constants K_b collected and calculated from the good linear relationship are listed in Table 2. The K_b values suggest a relatively moderate binding of compounds to CT DNA. The K_b values of Ln(III) complexes are higher than that of ligand ($K_b = 1.55 \times 10^4\ M^{-1}$) suggesting that ligand presents higher affinity to CT DNA, when it is coordinated to Ln(III). The higher binding affinity of Ln(III) complex is probably attributed to the extension of the π system of the intercalated ligand, which leads to a planar area greater than that of the free ligand, so the coordinated ligand penetrates more deeply into and stacks more strongly with DNA base pairs. As for Ln(III) complexes, the K_b values of Pr(III) complex ($K_b = 2.67 \times 10^4\ M^{-1}$) and Nd(III) complex ($K_b = 2.60 \times 10^4\ M^{-1}$) are approximately equal, which show that the binding strength of Pr(III) complex is equivalent to that of Nd(III) complex. The K_b values obtained here are as large as that reported for the other similar complexes whose binding constants have been found to be in the order of 10^4 M [46].

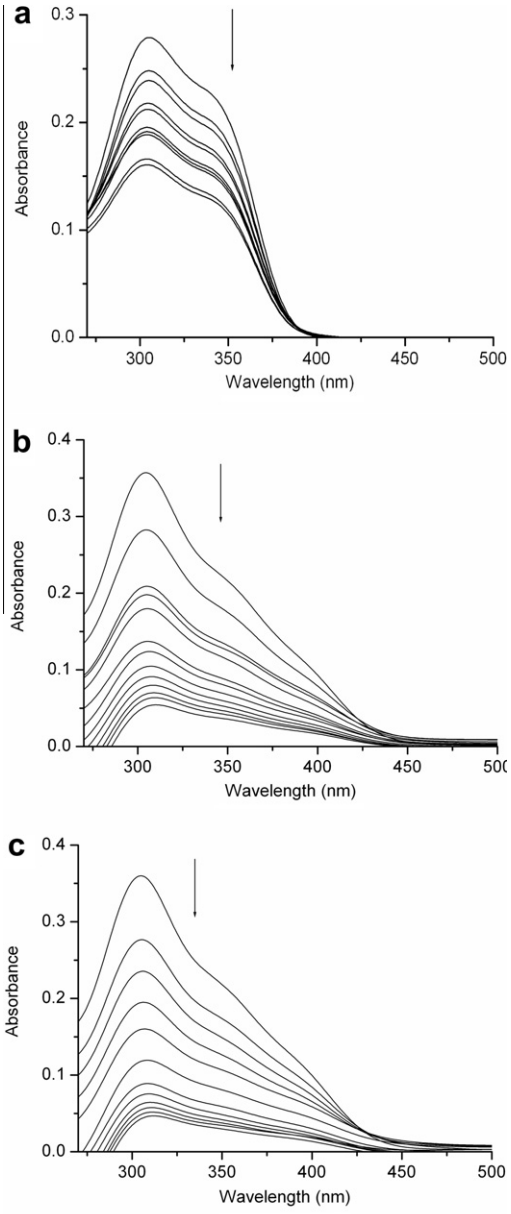

Fig. 6. UV spectra of investigated compounds ([compound] = 1×10^{-5} M) (a) ligand, (b) Pr(III) complex and (c) Nd(III) complex, in 5 mmol Tris–HCl buffer solution (pH 7.20) containing 50 mmol NaCl in the presence of CT DNA at increasing amounts. The arrows show the changes upon increasing amounts of CT DNA.

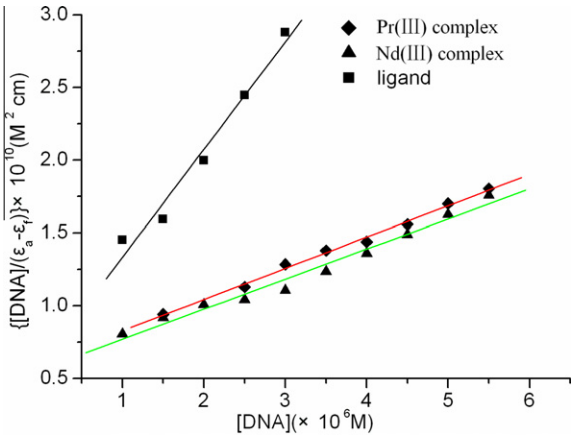

Fig. 7. Plots of [DNA]/($\varepsilon_a - \varepsilon_f$) vs. [DNA] for the titration of the investigated compounds. Tests were performed in the conditions of 5 mmol Tris–HCl buffer containing 50 mmol NaCl at 298 K.

3.3.3. EB–DNA quenching assay

The DNA-binding modes of compound are further monitored by fluorescent EB displacement assay. It is well known that EB can emit intense fluorescence due to strong intercalation nonspecifically between DNA base pairs [47,48]. Competitive binding of other drugs to DNA and EB will result in displacement of bound EB and decrease in the fluorescence intensity. The fluorescence-based competition technique can provide indirect evidence for the DNA binding mode. The fluorescence emission intensity of DNA–EB system decreased dramatically upon the increasing amounts of ligand and Ln(III) complexes. The observed quenching of DNA–EB fluorescence for all the compounds suggests that they can displace EB from the DNA–EB complex and can interact with CT DNA probably by the intercalative mode [49]. Stern–Volmer equation was used to determine the fluorescent quenching mechanism [50]. Quenching data K_{SV} is given by the ratio of the slope to the intercept in the plots of F_0/F versus [Q] (Fig. 8) and listed in Table 2. As shown, the data of K_{SV} are $5.36 \times 10^3\ M^{-1}$ for ligand, $1.65 \times 10^4\ M^{-1}$ for Pr(III) complex and $1.34 \times 10^4\ M^{-1}$ for Nd(III) complex, accordingly, the data of K_q calculated are $2.978 \times 10^{13}\ M^{-1}s^{-1}$ for ligand, $9.167 \times 10^{13}\ M^{-1}s^{-1}$ for Pr(III) complex and $7.444 \times 10^{13}\ M^{-1}s^{-1}$ for Nd(III) complex, respectively, when the value of τ_0 is taken as $1.8 \times 10^{-9}\ M^{-1}s^{-1}$ [45]. All of the current values of K_q for ligand and Ln(III) complexes are much greater than that of $K_{q(max)}$ ($2.0 \times 10^{10}\ M^{-1}s^{-1}$), the maximum quenching rate constant of bimolecular diffusion collision, which are indicative of static types of quenching mechanisms arisen from the formations of dark complexes between the fluorophores and quenching agents [51,52]. The data show that the interaction of the Ln(III) complexes with DNA is stronger than that of the free ligand, which is consistent with the viscosity titration and UV–Vis spectroscopy study results. Since these changes indicate only one kind of quenching process, it may be concluded that the Ln(III) complexes and free ligand bind to DNA via the same mode (intercalation mode).

3.3.4. CD spectroscopy

CT DNA in the B conformation shows two conservative CD bands, a positive band at 275 nm due to base stacking and a negative band at 245 nm due to right handed helicity [53]. These bands are sensitive towards binding of any small molecule or drug and hence can be exploited to investigate the binding of small molecules to DNA [54].CD spectroscopy was used to probe the global

Table 2
Parameters of K_b, K_{SV}, IC_{50} ($OH^{\cdot}$ and $O_2^{-\cdot}$) for ligand and Ln(III) complexes.

Compound	K_b (M^{-1})	K_{SV} (M^{-1})	K_q ($M^{-1}s^{-1}$)	IC_{50} (μM) for $HO^{\cdot}$	IC_{50} (μM) for $O_2^{-\cdot}$
ligand	$1.55(\pm0.09)\times10^4$	$5.36(\pm0.28)\times10^3$	2.978×10^{13}	42.59 ± 2.53	45.82 ± 1.81
Pr(III) complex	$2.67(\pm0.03)\times10^4$	$1.65(\pm0.04)\times10^4$	9.167×10^{13}	30.09 ± 2.46	24.41 ± 2.63
Nd(III) complex	$2.60(\pm0.05)\times10^4$	$1.34(\pm0.05)\times10^4$	7.444×10^{13}	33.25 ± 1.86	29.52 ± 3.11

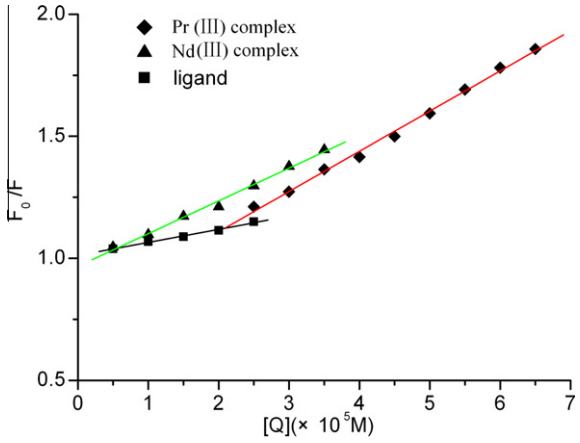

Fig. 8. Stern–Volmer plot of the fluorescence titration data of the investigated compounds. Tests were performed in the conditions of 5 mmol Tris–HCl buffer containing 50 mmol NaCl at 298 K. C_{DNA} = 4 μM (nucleotides), C_{EB} = 0.32 μM; λ_{ex} = 525 nm, λ_{em} = 587 nm.

changes in the DNA conformation induced by the complexes. Simple groove binding and electrostatic interactions of small molecules lead to no perturbation or marginal perturbations in these two CD bands of B-DNA. On the other hand, the major feature of CD spectra is the increase in the ellipticity for both bands of CT DNA, which is an indication of a typical intercalation involving π–π^* stacking and stabilization of the right-handed B form of CT DNA [55,56]. Fig. 9 shows the CD spectra obtained as a function of loading into CT DNA for Ln(III) complexes. There is not much change in the position of two bands at 245 nm and 275 nm, only the intensity of the bands increases upon addition of the complexes. This indicates that both Ln(III) complexes might interact with the DNA double strands by the intercalative mode between the base pairs of DNA strands without any significant change in the right handed helicity of CT DNA.

3.3.5. Cyclic voltammetry

The changes observed in the cyclic voltammogram of a small molecule upon addition CT DNA can provide a useful complement to spectroscopic methods for the molecule–DNA interaction [57] since the electrochemical potential of the molecule will shift positively when the molecule intercalates into DNA double helix, and it will shift into a negative direction, if the molecule is bound to DNA by an electrostatic interaction [21,58]. Additionally, when more potentials than one exist, a positive shift of E_{p1} and a negative shift of E_{p2} imply that the molecule can bind to DNA by both intercalation and electrostatic interaction [59]. No new redox peaks appeared after the addition of CT DNA to each complex, but the current of all the peaks decreased significantly, suggesting the existence of an interaction between each complex and CT DNA. The decrease in current can be explained in terms of an equilibrium mixture of free and DNA-bound complex to the electrode surface [60].

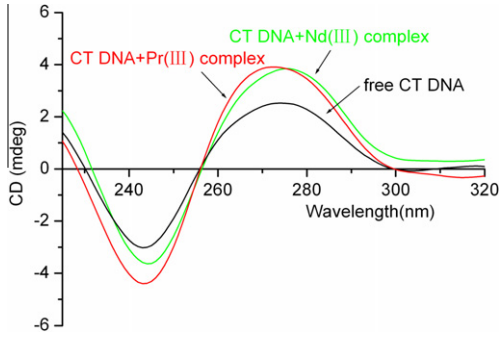

Fig. 9. Circular Dichroic spectra of CT DNA in the absence and presence of Ln(III) complexes with [complex]/[DNA] = 0.5.

The cyclic voltammograms of Ln(III) complexes in the absence or presence of CT DNA showed that no new redox peaks appeared after the addition of CT DNA to the complexes, but the current intensity of the negative peaks decreased significantly (see supporting information Fig. S1). The above phenomenon suggested that the existence of the interaction between Ln(III) complexes and CT DNA, and can be explained in terms of an equilibrium mixture of free and DNA-bound complex to the electrode surface [59]. It can be observed (Fig. S1) that for increasing amounts of CT DNA, the cathodic potential E_{pc} shows a positive shift up to about −894 mV (ΔE_{pc} = +50 mV for Pr(III) complex and +12 mV for Nd(III) complex) and the anodic potential E_{pa} presents little shift. These positive shifts of the potentials may suggest the existence of intercalation between complexes and CT DNA as the most possible interaction mode [42,61]. The electrochemical parameters of Ln(III) complexes in the absence and presence of 30 μM DNA are listed in Table 3. The values of ΔE_p > 212 mV reflect the redox processes of the free and DNA-bound complexes to be less reversible [62].

3.4. Cleavage plasmid pBR322 DNA

Petra Drevensek and coworkers reported a new quinolone–Cu complex that shows efficient DNA cleavage activity in the absence and presence of peroxide [63]. Hence we were also interested to assess the chemical nuclease activities of these two Ln(III) complexes for DNA strand scission. In our research, pBR322 DNA was incubated with the complexes under the reaction conditions and the cleavage reaction can be monitored by gel electrophoresis.

3.4.1. Chemical nuclease activity

When circular pBR322 DNA is subjected to electrophoresis, relatively fast migration will be observed for the intact supercoiled form (Form I). If scission occurs on one strand (nicking), the supercoiled form will relax to generate a slower-moving nicked form (Form II). If both strands are cleaved, a linear form (Form III) that migrates between Form I and Form II will be generated[64,65].

To assess the DNA cleavage ability of Ln(III) complexes, supercoiled pBR322 DNA (20 μM) was incubated with 20–100 μM of all complexes in TBE buffer for 13 h without the addition of a reductant [66]. Control experiments show that the free ligand, $Pr(NO_3)_3{\cdot}6H_2O$ and $Nd(NO_3)_3{\cdot}6H_2O$ are cleavage inactive (see supporting information Fig. S2). The SC DNA (form I) was cleaved by both Ln(III) complexes, especially when the concentrations of the

Table 3
CV data of Ln(III) complexes.

	CV data						
	E_{pa} (V)	E_{pc} (V)	ΔE_p (mV)	E° (V)	I_{pa} (μA)	I_{pc} (μA)	I_{pc}/I_{pa}
Pr(III) complex	−0.583	−0.940	357	−0.811	0.36	3.83	10.70
Pr(III) complex–DNA	−0.577	−0.890	313	−0.738	0.16	2.73	16.75
Nd(III) complex	−0.676	−0.906	230	−0.791	0.50	4.54	9.08
Nd(III) complex–DNA	−0.671	−0.894	240	−0.775	0.55	3.81	6.95

two complexes are above 60 μM (see supporting information Fig. S3). The results indicate that the DNA cleavage activity of Ln(III) complexes is obviously complex concentration dependent. At the concentration of 60 μM, Ln(III) complexes can almost promote the complete conversion of plasmid pBR 322 from Form I to Form II (lane 4).

3.4.2. Mechanistic studies

The DNA cleavage activity of the complexes has been studied in the presence of several additives to understand the mechanistic pathway involved in the DNA cleavage reaction. From Fig. 10, we can see that no obvious inhibitions are observed for the two Ln(III) complexes in the presence of NaN_3 (lane 3) and L-Histidine (lane 4), the results rule out the possibility of DNA cleavage by the singlet oxygen or a singlet oxygen-like entity. The addition of DMSO (lane 5), EtOH (lane6) partly diminishes the nuclease activity of the Ln(III) complexes which is indicative of the involvement of hydroxyl radical in the cleavage process.

3.5. Antioxidation properties

Owning to the ligand and its Ln(III) complexes exhibit good DNA binding affinity, it is considered worthwhile to study the antioxidant activity of these compounds. Generation of reactive oxygen species (ROS) is a normal process in the life of aerobic organisms. It has been estimated that free radical-induced DNA damage in humans is at biologically relevant levels, with approximately 10^4 DNA bases being oxidatively modified per cell per day. Oxidative damage to DNA has been suggested to contribute to aging and various diseases including cancer and chronic inflammation [67]. ($O_2^{-\cdot}$) and ($HO^\cdot$) are two clinically important reactive oxygen species in the human body [29]. They are produced in most organ systems and participate in various physiological and pathophysiological processes such as carcinogenesis, aging, viral infection, inflammation, and others [68]. Consequently, in this paper, the ligand and its Ln(III)complexes studied for their antioxidant activity by comparing their scavenging effects on $O_2^{-\cdot}$ and $HO^\cdot$.

Fig. 11a shows the plots of hydroxyl radical scavenging effect (%) for ligand and Ln(III) complexes, which are concentration-dependant. As shown in Table 2. The average suppression ratio of the ligand is the poorest in all the compounds and Pr (III) complex is the most effective one, which indicate that because of the formation of coordination compounds, the scavenger effect can be enhanced.Fig. 11b shows the plots of superoxide radical scavenging effects (%) for ligand and Ln(III) complexes, which are also concentration-dependant. The data of the suppression ratio for $O_2^{-\cdot}$ are listed in Table 2. The average suppression ratio of the free ligand for $O_2^{-\cdot}$ is the least in all compounds and Pr(III) complex is the most effective one. The order of the suppression ratio of the tested compounds for $HO^\cdot$ and $O_2^{-\cdot}$ is Pr(III) complex > Nd(III) complex > ligand.From Table 2, we can easily find that Ln(III) complexes exhibit considerable scavenging activity due to the chelation of organic molecules to the lanthanide ions. It is reported that the value of IC_{50} of ascorbic acid (Vc), a standard agent for non-enzymatic reaction, for $HO^\cdot$ is 1.537 mg cm^{-3} (8.727 mmol), and the scavenging effect of Vc for $O_2^{-\cdot}$ is only 25% at 1.75 mg cm^{-3} (9.94 mmol) in vitro [69]. So it is pronounced that ligand and Ln(III) complexes investigated here are less effective inhibitor than the other similar complexes [70], but have

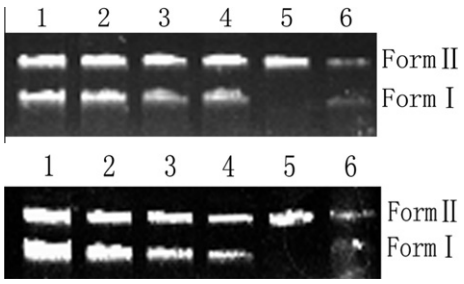

Fig. 10. Agarose gel showing cleavage of pBR322 DNA (0.1 μg/μL) incubated with 0.1 mM Pr(III) complex (a) and Nd(III) complex (b) for 5 h at 37 °C in a TBE buffer at pH 8.3. Lane 1: DNA control; lane 2: DNA + Ln(III) complex; lane 3: DNA + Ln(III) complex + 100 mM NaN_3; lane 4: DNA + Ln(III) complex + 100 mM L-Histidine; lane 5: DNA + Ln(III) complex + 2μL DMSO; lane 6: DNA + Ln(III) complex + 2μL EtOH.

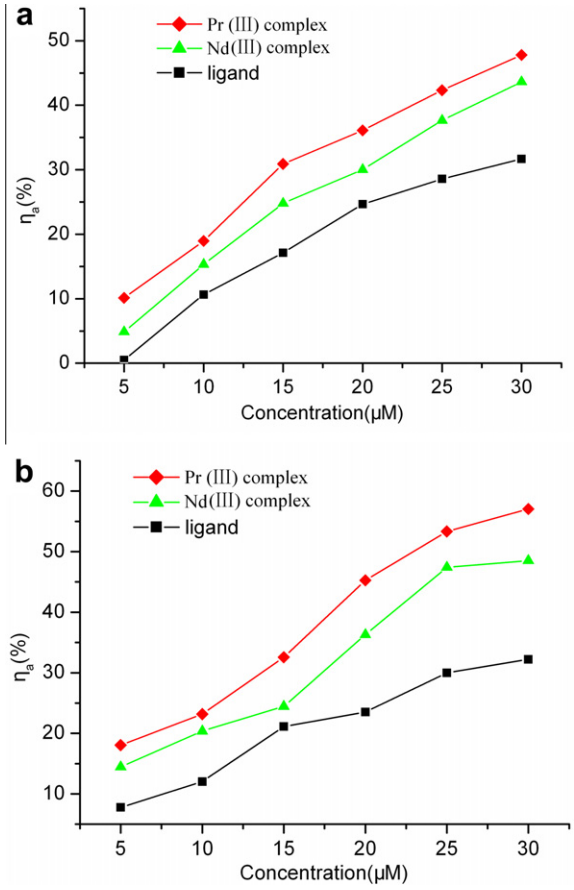

Fig. 11. Plots of antioxidation properties for the investigated compounds. (a) Represent the hydroxyl radical scavenging effect (%) for the investigated compounds. (b) Represents the superoxide radical scavenging effect (%) for the investigated compounds.

much stronger scavenging abilities for $HO^{\bullet}$ and $O_2^{-\cdot}$ than ascorbic acid (Vc). Endowed with antioxidative properties, these DNA binders may be effective inhibitors of the formation of a DNA/TBP complex topoisomerases [71–73].

4. Conclusions

Two new water-soluble Ln(III) complexes of acylhydrazone ligand derived from ofloxacin were synthesized and characterized. The DNA binding mode of Ln(III) complexes and ligand with CT DNA were studied via spectra, CV and viscosity measurement. The experiment results suggest that ligand and its Ln(III) complexes bind to DNA via intercalation mode, and Ln(III) complexes have higher binding ability than free ligand. We also find that both Ln(III) complexes can effectively cleave plasmid DNA without addition of external agents. DNA cleavage mechanism studies show that the Ln(III) complexes examined here may be capable of promoting DNA cleavage through hydrolytic DNA damage pathways. Moreover, Ln(III) complexes have better antioxidant activity than pure ligand.

Acknowledgments

Thanks Henan Province Science and Technology Key Project (112102310539), Natural Science Foundation of Henan Province (2010B150029) and Xuchang University for financial support.

Appendix A. Supplementary material

CCDC 768805 and 768806 contain the supplementary crystallographic data for complexes Pr(III) and Nd(III). These data can be obtained free of charge from The Cambridge Crystallographic Data Centre via www.ccdc.cam.ac.uk/data_request/cif. Supplementary data associated with this article can be found, in the online version, at doi:10.1016/j.ica.2011.12.031.

References

[1] D.S. Sigman, A. Mazumder, D.M. Perrin, Chem. Rev. 93 (1993) 2295.
[2] C.J. Burrows, J.G. Muller, Chem. Rev. 98 (1998) 1109.
[3] J.A. Cowan, Curr. Opin. Chem. Biol. 5 (2001) 634.
[4] P. Molenveld, J.F.J. Engbersen, D.N. Reinhoudt, Chem. Soc. Rev. 29 (2000) 75.
[5] C. Liu, M.. Wang, T. Zhang, H. Sun, Coord. Chem. Rev. 248 (2004) 147.
[6] M. Komiyama, N. Takida, H. Shigekawa, Chem. Commun. 16 (1999) 1443.
[7] H.T. Chifotides, K.R. Dunbar, Acc. Chem. Res. 38 (2005) 146.
[8] M. Demeunynck, C. Bailly, W.D. Wilson (Eds.), Wiley-VCH, Weinheim, 2003.
[9] R.W.Y. Sun, D.L. Ma, E.L.M. Wong, C.M. Che, Dalton Trans. (2007) 4884.
[10] C. Moucheron, New J. Chem. 33 (2009) 235.
[11] I. Turel, Coord. Chem. Rev. 232 (2002) 27.
[12] A.R.A. Abd-Allah, B.B. Gannam, F.M.A. Hamada, Pharm. Res. 42 (2000) 145.
[13] W.E. Sanders Jr., Clin. Infect. Dis. 14 (1992) 539.
[14] L. Savanini, L. Chiasserini, A. Gaeta, C. Pellerano, Bioorg. Med. Chem. 10 (2002) 2193.
[15] E. Ochiai, Bioinorganic Chemistry, Allyn and Bacon, Boston, 1977.
[16] J.A. Anten, D. Nicholis, J.M. Markpoulos, O. Markopoulou, Polyhedron 6 (1987) 1075.
[17] I.A. Tossadis, C.A. Bolos, P.N. Aslanidis, G.A. Katsoulos, Inorg. Chim. Acta 133 (1987) 275.
[18] J.C. Craliz, J.C. Rub, D. Willis, J. Edger, Nature 34 (1955) 176.
[19] Y.Z. Cai, Q. Luo, M. Sun, H. Corke, Life Sci. 74 (2004) 2157.
[20] K.E. Heim, A.R. Tagliaferro, D.J. Bobilya, J. Nutr. Biochem. 13 (2002) 572.
[21] M.T. Carter, M. Rodriguez, A.J. Bard, J. Am. Chem. Soc. 111 (1989) 8901.
[22] A. Wolf, G.H. Shimer, T. Meehan, Biochemistry 26 (1987) 6392.
[23] M. Howe-Grant, K.C. Wu, W.R. Bauer, S.J. Lippard, Biochemistry 15 (1976) 4339.
[24] M.R. Eftink, C.A. Ghiron, Anal. Biochem. 114 (1981) 199.
[25] C.C. Winterbourn, Biochem. J. 198 (1981) 125.
[26] C.C. Winterbourn, Biochem. J. 182 (1979) 625.
[27] G.M. Sheldrick, SHELXTL v5, Reference Manual, Siemens Analytical X-ray Systems, Madison, WI, 1996.
[28] F.D. Lewis, S.V. Barancyk, J. Am. Chem. Soc. 111 (1989) 8653.
[29] N. Raman, A. Kulandaisamy, K. Jeyasubramanian, J. Ind. Chem. 41A (2002) 942.
[30] B.D. Wang, Z.Y. Yang, D.W. Zhang, Y. Wang, Spectrochim. Acta, Part A 63 (2006) 213.
[31] S. Sagdinc, S. Bayari, J. Mol. Struct. 691 (2004) 107.
[32] B. Macias, M.V. Villa, M. Sastre, A. Castineiras, J. Borras, J. Pharm. Sci. 91 (2002) 2416.
[33] B. Macias, M.V. Villa, I. Rubio, A. Castineiras, J. Borras, J. Inorg. Biochem. 84 (2001) 163.
[34] P. Drevensek, J. Kosmrlj, G. Giester, T. Skauge, E. Sletten, K. Sepcic, I. Turel, J. Inorg. Biochem. 100 (2006) 1755.
[35] I. Turel, J. Kljun, F. Perdih, E. Morozova, V. Bakulev, N. Kasyanenko, J.A.W. Byl, N. Osheroff, Inorg. Chem. 49 (2010) 10750.
[36] S. Mahadevan, M. Palaniandavar, Inorg. Chem. 37 (1998) 693.
[37] A.B. Tossi, J.M. Kelly, Photochem. Photobiol. 9 (1989) 545.
[38] J.G. Liu, Q.L. Zhang, X.F. Shi, L.N. Ji, Inorg. Chem. 40 (2001) 5045.
[39] S. Satyanarayana, J.C. Dabrowiak, J.B. Chaires, Biochemistry 32 (1993) 2573.
[40] R.D. Snyder, Mutat. Res. 623 (2007) 72.
[41] A.M. Pyle, J.P. Rehmann, R. Meshoyrer, C.V. Kumar, N.J. Turro, J.K. Barton, J. Am. Chem. Soc. 111 (1989) 3053.
[42] E.C. Long, J.K. Barton, Acc. Chem. Res. 23 (1990) 271.
[43] J.K. Barton, A.T. Danishefsky, J.M. Goldberg, J. Am. Chem. Soc. 106 (1984) 2172.
[44] H.L. Lu, J.J. Liang, Z.Z. Zeng, P.X. Xi, X.H. Liu, F.J. Chen, Z.H. Xu, Transition Met. Chem. 32 (2007) 564.
[45] J.Z. Wu, B.H. Ye, L. Wang, L.N. Ji, J.Y. Zhou, R.H. Li, Z.Y. Zhou, J. Chem. Soc., Dalton Trans. 8 (1997) 1395.
[46] M. Xu, Z.R. Ma, L. Huang, F.J. Chen, Z.Z. Zeng, Spectrochim. Acta, Part A 78 (2011) 503.
[47] W.D. Wilson, L. Ratmeyer, M. Zhao, L. Stekowshi, D. Boykin, Biochemistry 32 (1993) 4098.
[48] R.F. Pasternack, M. Caccam, B. Keogh, T.A. Stephenson, A.P. Williams, E.J. Gibbs, J. Am. Chem. Soc. 113 (1991) 6835.
[49] C.V. Kumar, J.K. Barton, N.J. Turro, J. Am. Chem. Soc. 107 (1985) 5518.
[50] D. Suh, J.B. Chaires, Bioorg. Med. Chem. 3 (1995) 723.
[51] Y.C. Liu, Z.Y. Yang, J. Du, X.J. Yao, R.X. Lei, X.D. Zheng, Chem. Pharm. Bull. 56 (2008) 443.
[52] Y.C. Liu, Z.Y. Yang, J. Du, X.J. Yao, R.X. Lei, X.D. Zheng, J.N. Liu, H.S. Hu, H. Li, Immunobiology 213 (2008) 651.
[53] W.C. Johnson, CD of nucleic acids, in: K. Nakanishi, N. Berova, R.W. Woody (Eds.), VCH, 1994, New York, p. 523.
[54] B. Norden, F. Tjerneld, Biopolymers 21 (1982) 1713.
[55] N. Shahabadi, S. Kashanian, M. Purfoulad, Spectrochim. Acta, Part A 72(2009) 757.
[56] E.K. Efthimiadou, N. Katsaros, A. Karaliota, G. Psomas, Inorg. Chim. Acta 360 (2007) 4093.
[57] M.T. Carter, A.J. Bard, J. Am. Chem. Soc. 109 (1987) 7528.
[58] S.S. Zhang, S.Y. Niu, B. Qu, G.F. Jie, H. Xu, C.F. Ding, J. Inorg. Biochem. 99 (2005) 2340.
[59] K. Jiao, Q. Wang, W. Sun, G.F. Jie, H. Xu, C.F. Ding, J. Inorg. Biochem. 99 (2005) 1369.
[60] S. Tabassum, S. Parveen, F. Arjmand, Acta Biomaterials 1 (2005) 677.
[61] G. Psomas, J. Inorg. Biochem. 102 (2008) 1798.
[62] P.U. Maheswari, M. van der Ster, S. Smulders, S. Barends, G.P. van Wezel, C. Massera, S. Roy, H. den Dulk, P. Gamez, J. Reedijk, Inorg. Chem. 47 (2008) 3719.
[63] P. Drevensek, T. Zupancic, B. Pihlar, R. Jerala, U. Kolitsch, A. Plaper, I. Turel, J. Inorg. Biochem. 99 (2005) 432.
[64] X.W. Liu, J. Li, H. Li, K.C. Zheng, H. Chao, L.N. Ji, J. Inorg. Biochem. 100 (2006) 385.
[65] H. Chao, W.J. Mei, Q.W. Huang, L.N. Ji, J. Inorg. Biochem. 92 (2002) 165.
[66] M.S. Deshpande, A.A. Kumbhar, A.S. Kumbhar, M. Kumbharkar, H. Pal, U.B. Sonowane, R.R. Joshi, Bioconjugate Chem. 20 (2009) 447.
[67] K. Tsai, T.G. Hsu, K.M. Hsu, H. Cheng, T.Y. Liu, C.F. Hsu, C.W. Kong, Free Radical Biol. Med. 31 (2001) 1465.
[68] A.M. Pyle, J.P. Rehmann, R. Meshoyrer, C.V. Kumar, N.J. Turro, J.K. Barton, J. Am. Chem. Soc. 111 (1989) 3051.
[69] R.G. Xing, H.H. Yu, S. Liu, C.V. Kumar, N.J. Turro, J.K. Barton, Bioorg. Med. Chem. 13 (2005) 1387.
[70] Y. Li, Z.Y. Yang, M.F. Wang, Eur. J. Med. Chem. 44 (2009) 4585.
[71] S.Y. Chiang, J. Welch, F.J. Rauscher, T.A. Beerman, Biochemistry 33 (1994) 7033.
[72] J.M. Woynarowski, M. Mchugh, R.D. Sigmund, T.A. Beerman, Mol. Pharmacol. 35 (1989) 177.
[73] A.Y. Chen, C. Yu, B. Gatto, L.F. Liu, Proc. Natl. Acad. Sci. USA 90 (1993) 8131.